

Article

# Evaluation of Functionalized Porous Titanium Implants for Enhancing Angiogenesis *in Vitro*

Laura Roland <sup>1,2</sup>, Samantha Backhaus <sup>1</sup>, Michael Grau <sup>1,2</sup>, Julia Matena <sup>1,2</sup>, Michael Teske <sup>3</sup>, Martin Beyerbach <sup>4</sup>, Hugo Murua Escobar <sup>1,2</sup>, Heinz Haferkamp <sup>5</sup>, Nils-Claudius Gellrich <sup>6</sup> and Ingo Nolte <sup>1,\*</sup>

<sup>1</sup> Small Animal Clinic, University of Veterinary Medicine Hannover, Foundation, Hannover D-30559, Germany; laura.roland@tiho-hannover.de (L.R.); samanthabackhaus@live.de (S.B.); michael.grau@tiho-hannover.de (M.G.); julia.matena@tiho-hannover.de (J.M.); hugo.murua.escobar@med.uni-rostock.de (H.M.E.)

<sup>2</sup> Division of Medicine Clinic III, Hematology, Oncology and Palliative Medicine, University of Rostock, Rostock D-18057, Germany

<sup>3</sup> Institute for Biomedical Engineering, Rostock University Medical Center, Rostock D-18119, Germany; michael.teske@uni-rostock.de

<sup>4</sup> Institute for Biometry, Epidemiology and Information Processing, University of Veterinary Medicine Hannover, Foundation, Hannover D-30559, Germany; martin.beyerbach@tiho-hannover.de

<sup>5</sup> Institut fuer Werkstoffkunde, Leibniz Universitaet Hannover, Garbsen D-30823, Germany; haferkamp@iw.uni-hannover.de

<sup>6</sup> Clinic for Cranio-Maxillo-Facial Surgery, Hannover Medical School, Hannover D-30625, Germany; gellrich.nils-claudius@mh-hannover.de

\* Correspondence: ingo.nolte@tiho-hannover.de; Tel.: +49-511-953-6400

Academic Editor: Alina Maria Holban

Received: 3 March 2016; Accepted: 18 April 2016; Published: 22 April 2016

**Abstract:** Implant constructs supporting angiogenesis are favorable for treating critically-sized bone defects, as ingrowth of capillaries towards the center of large defects is often insufficient. Consequently, the insufficient nutritional supply of these regions leads to impaired bone healing. Implants with specially designed angiogenic supporting geometry and functionalized with proangiogenic cytokines can enhance angiogenesis. In this study, Vascular Endothelial Growth Factor (VEGF) and High Mobility Group Box 1 (HMGB1) were used for incorporation into poly- $\epsilon$ -caprolactone (PCL)-coated porous titanium implants. Bioactivity of released factors and influence on angiogenesis of functionalized implants were evaluated using a migration assay and angiogenesis assays. Both implants released angiogenic factors, inducing migration of endothelial cells. Also, VEGF-functionalized PCL-coated titanium implants enhanced angiogenesis *in vitro*. Both factors were rapidly released in high doses from the implant coating during the first 72 h.

**Keywords:** titanium; angiogenesis; VEGF; HMGB1; functionalized implants; PCL

## 1. Introduction

Angiogenesis plays a major role in healing of critically-sized bone defects [1]. The importance of blood vessel formation for bone repair and building of a skeleton structure was already described in the 18th century as reviewed by Carano *et al.* [2]. Thereby, vasculature ensures a sufficient supply of soluble nutrients, cytokines, cells, and oxygen to all tissues [3]. Consequently, insufficient blood supply is one of the major reasons for impaired bone healing [4]. Such insufficient blood vessel ingrowth is often seen in large oral and maxillofacial defects, resulting from accidents, bone inflammation, or neoplasia, often leading to a non-union of the bone [5–7].

Accordingly, an efficient treatment of those critically sized bone defects requires specially designed and functionalized implants. Currently, the gold-standard for treating these defects are autologous

bone transplants which have unfortunately limited availability and are accompanied by donor side morbidity as well as high costs [8–10].

Titanium is a well-established implant material characterized by high biocompatibility and resistance to corrosion [11–13]. Furthermore it has good initial stability and is well tolerated by tissues as it does not evoke foreign body reactions [14]. In general, a porous implant structure is favorable for improving ingrowth of blood vessels and bone, as well as for overcoming the mismatch between the Young's modulus between bone (10–30 GPa) and titanium (about 110 GPa for Ti6Al4V), which can lead to stress-shielding and, consequently, to loosening of the implant-bone interface [15,16]. Porous titanium implants are proven to be promising for treating large bone defects as they have an osteoconductive effect [17]. SLM<sup>®</sup>-made (SLM Solutions GmbH, Luebeck, Germany) porous titanium implants with a pore size of 600 µm and a poly-ε-caprolactone (PCL) coating were examined and found to be promising for treating critically-sized bone defects [18].

In previous studies, a positive effect of proangiogenic factors loaded scaffolds on vascularization was confirmed [19–21]. For functionalization of titanium implants with proangiogenic factors, a PCL coating is promising, as it has proven to be biocompatible and to enable growth of osteoblasts on its surface [18,22]. PCL, as a coating and drug delivery device, has come to our focus as PCL has favorable degradation kinetics and its bio- and cytocompatibility have been confirmed by several studies [23–25]. Furthermore, its high permeability to many drugs and its ability to be fully excreted by the body make it attractive for drug delivery [22].

Vascular Endothelial Growth Factor (VEGF) is a potent angiogenic regulator. VEGF has a chemotactic effect on endothelial cells *in vitro* and has been proven to induce angiogenesis *in vivo* in model systems, such as the rabbit cornea or the chorioallantoic membrane [26]. Furthermore, it functions directly chemotactically on osteoblasts and osteoclasts [27]. High Mobility Group Box 1 (HMGB1) is a proangiogenic factor which mediates its effect as ligand of the receptor for advanced glycation end products (RAGE) or toll-like receptors TLR2 and TLR4 [28,29].

V2a Kit<sup>™</sup> (TCSCellworks, Buckingham, UK) has been proven to be a suitable method for evaluating the influence of different implant materials and coatings on angiogenesis *in vitro* [18].

The aim of the present study was to prove the bioactivity of VEGF and HMGB1 after incorporation into implants and their proangiogenic effect. Also, cytokines were tested directly using an angiogenesis assay to rule out any negative effect of the implant or the coating itself. Additionally, the releasing progress of these cytokines from PCL-coated titanium implants was examined.

## 2. Results

### 2.1. PCL Coating Thickness and Mass

As an even coating of the implant is favorable for controlled drug release, cross-section polishes of the titanium scaffolds were prepared to determine the thickness of PCL coatings (Table 1). In order to visualize the coating, environmental scanning electron microscopy (ESEM) was performed (Quanta FEG 250, FEI, Eindhoven, The Netherlands) (Figure 1). Three different samples were examined, which all were coated during different coating processes. The measured middle coating thickness was between 11.4 and 15.5 µm. Thus, a high standard deviation for all samples was observed which was at least approximately half of the determined PCL coating thickness. For the titanium scaffolds with HMGB1 loading, a higher standard deviation of approximately 2/3 of the coating thickness could be observed.

The PCL coating weight measurements amounted to  $0.305 \pm 0.065$  mg. With a standard deviation of around 20%, only a low standard deviation in mass measurements regarding the standard deviation of coating thickness could be detected. That is why we assume that the complicated and porous titanium scaffold structure causes the high thickness standard deviation.

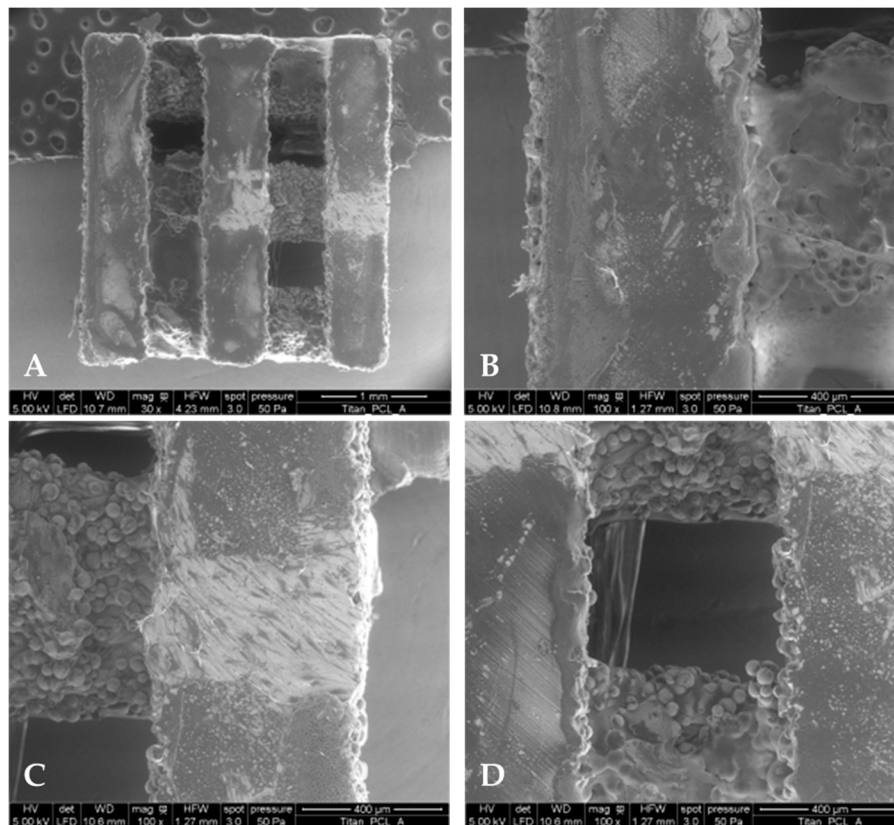


**Figure 1.** ESEM (environmental scanning electron microscopy) pictures (Quanta FEG 250, FEI, Eindhoven, The Netherlands) of PCL-coated titanium implant. The whole implant (A) was imaged as well as different parts of the implant (B–D). After fixing the implants, the scanning electron micrographs were performed at 50 Pa pressure, with moisturized atmosphere and an accelerating voltage of 5 kV (HV = high voltage; det = detector; LFD = large field detector; WD = working distance, HFE = horizontal field width, mag = magnification).

**Table 1.** PCL coating thickness of the *in vitro* tested Titanium Scaffolds ( $n = 3$ ).

Sample	Coating Thickness of PCL ( $\mu\text{m}$ )
Titanium-PCL	$11.6 \pm 6.2$
Titanium-PCL + VEGF	$11.4 \pm 7.3$
Titanium-PCL + HMGB1	$15.5 \pm 10.1$
Titanium-PCL + VEGF + HMGB1	$15.3 \pm 7.4$

## 2.2. Migration Assay

To prove bioactivity of growth factors being released from functionalized titanium implants, a migration assay with endothelial cells (GM7373) was performed. GM7373 cells showed significantly higher chemotaxis using supernatants from functionalized implants compared to the control DMEM (Dulbecco's Modified Eagle Medium) (Biochrom AG, Berlin, Germany) with 20% FCS (fetal calf serum) (PAA, Coelbe, Germany) or 0.1% FCS (Figure 2). Chemotaxis was significantly higher for DMEM with 20% than for DMEM with 0.1% FCS.

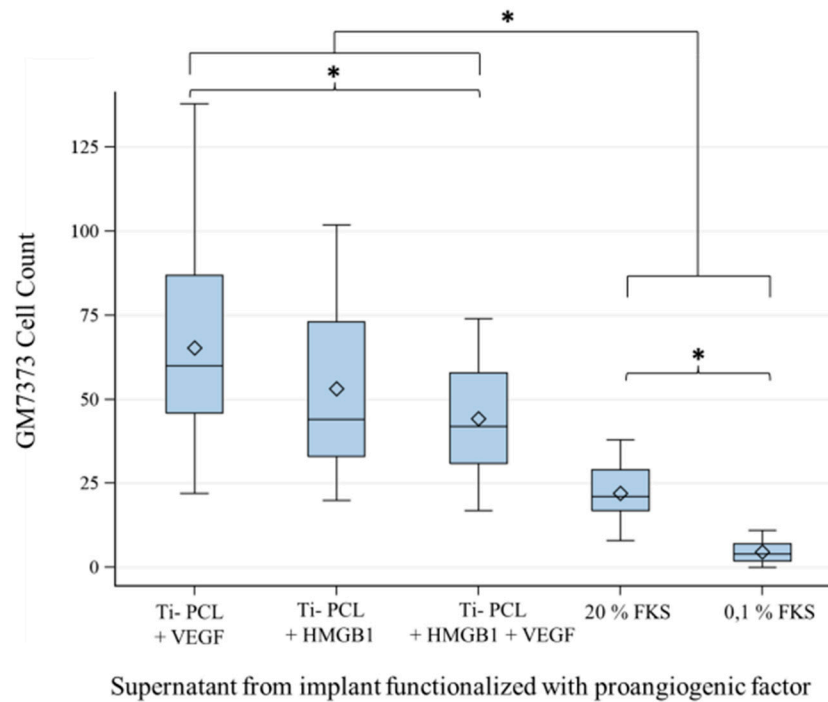


**Figure 2.** Migration Assay with GM7373 and supernatants from functionalized implants. Comparison of chemotactic behavior of the endothelial cell line (GM7373) using supernatants from implants functionalized with VEGF (vascular endothelial growth factor), HMGB1 (high mobility group box 1) and a combination of HMGB1/VEGF. All of the functionalized implants showed significantly higher chemotaxis than DMEM with 20% FCS or 0.1% FCS. VEGF was significantly more chemotactic than the combination of VEGF + HMGB1. *F*-test from the analyses of variance followed by pairwise multiple means comparisons with the Least Significant Difference test were used ( $p \leq 0.05$ ).

GM7373 showed the highest chemotaxis using supernatants of titanium implants functionalized with VEGF. Chemotaxis towards supernatants from VEGF-functionalized implants was significantly better than chemotaxis using supernatants of titanium implants functionalized with VEGF + HMGB1. There was no significant difference between HMGB1 and VEGF + HMGB1.

### 2.3. Angiogenesis Assay with Functionalized Titanium Implants

As migration assay only offers the opportunity of indirect testing of cell culture supernatants, an angiogenesis assay was performed. This offers the opportunity to prove functionalized implants directly in an *in vitro* cell culture model [18]. Tubuli sprouting was visible (Figure 3) and the characteristics Number of Junction (Figure 4), Number of Tubules (Figure 5), Total Tubule Length ( $\mu\text{m}$ ) (Figure 6), and Number of Nets (Figure 7) were evaluated for the different functionalized implants.

The most significant results for all of the mentioned characteristics were achieved by titanium implants functionalized with VEGF. Titanium implants functionalized with HMGB1 showed similar results as pure titanium implants and titanium implants coated with PCL. Significantly more junctions, tubules, and a higher tubule length could be detected for pure titanium implants compared to titanium implants coated with PCL.

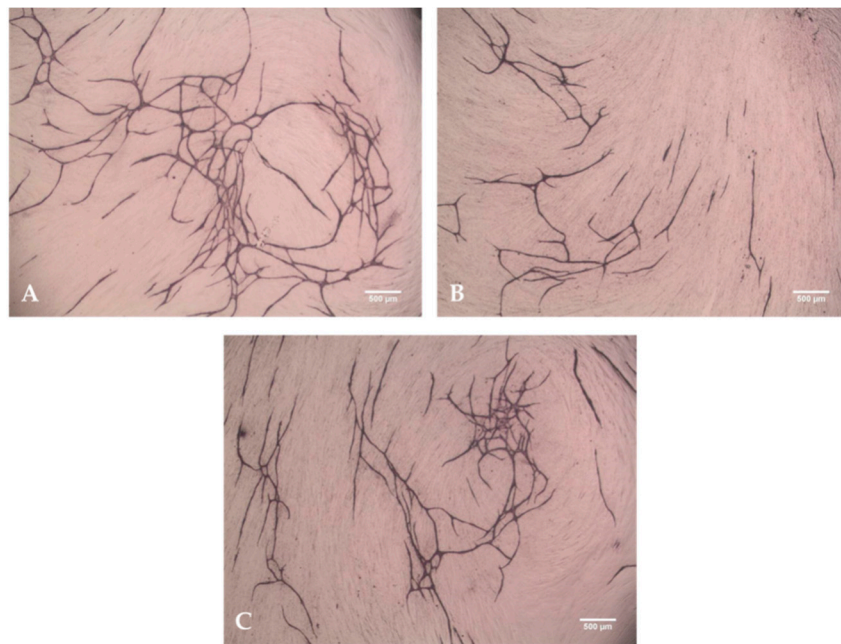


**Figure 3.** Tubuli and Nets visible after Angiogenesis Assay. After staining with BCIP/NBT-Substrate, tubuli and net-structures became visible. (A) Titanium implant functionalized with VEGF; (B) titanium implant functionalized with HMGB1; and (C) titanium implant functionalized with a combination of VEGF + HMGB1.

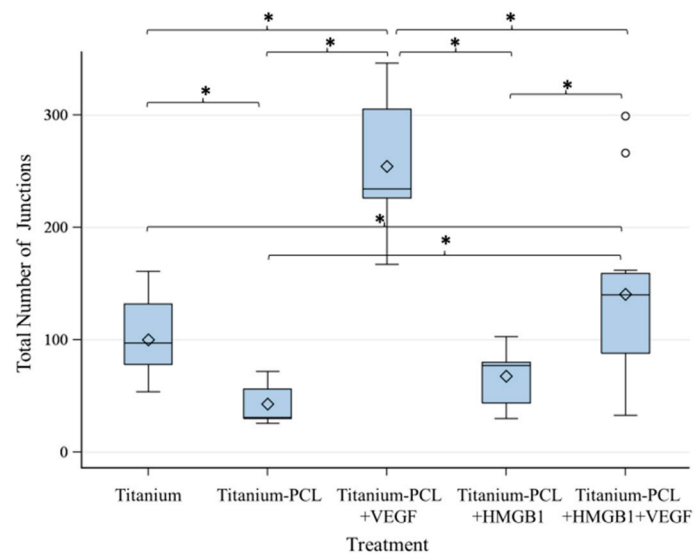


**Figure 4.** Number of Junctions built due to the investigated implant. VEGF-functionalized titanium-PCL implants showed significantly more junctions than all of the other implants. VEGF + HMGB1-functionalized titanium-PCL implants built significantly more junctions than pure titanium implants, titanium implants coated with PCL and HMGB1-functionalized titanium-PCL implants. Significantly more junctions could be seen in wells with pure titanium implants than in wells with titanium-PCL implants. *F*-test from the analyses of variance followed by pairwise multiple means comparisons with the Least Significant Difference test were used ( $p \leq 0.05$ ).

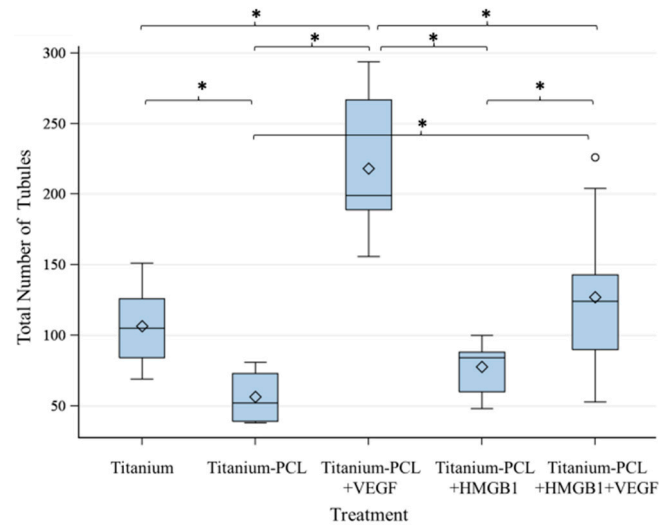


**Figure 5.** Number of Tubules built by investigated implants. VEGF-functionalized titanium-PCL implants built significantly more tubules than all of the other implants. VEGF + HMGB1-functionalized titanium-PCL implants showed significantly more tubules than titanium-PCL implants and HMGB1 functionalized titanium-PCL implants. Pure titanium implants showed better results than titanium-PCL implants. *F*-test from the analysis of variance followed by pairwise multiple means comparisons with the Least Significant Difference test were used ( $p \leq 0.05$ ).

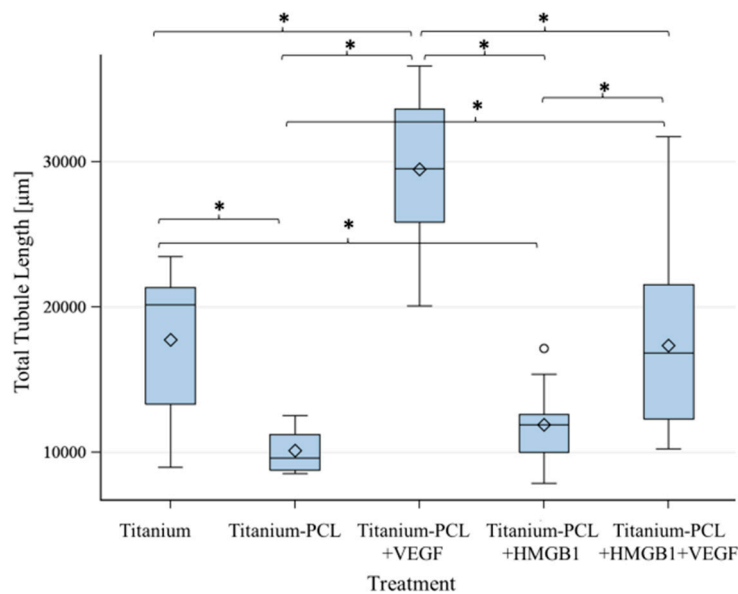


**Figure 6.** Total Tubule Length built by investigated implants. VEGF-functionalized titanium-PCL implants showed significantly the best results for the characteristic Total Tubule Length. VEGF + HMGB1-functionalized titanium-PCL implants showed a significantly higher Total Tubule Length than titanium-PCL implants and HMGB1-functionalized titanium-PCL implants, but comparable results to pure titanium implants. Pure titanium implants were significantly better than titanium-PCL implants and HMGB1-functionalized titanium-PCL implants. *F*-test from the analyses of variance followed by pairwise multiple means comparisons with the Least Significant Difference test were used ( $p \leq 0.05$ ).

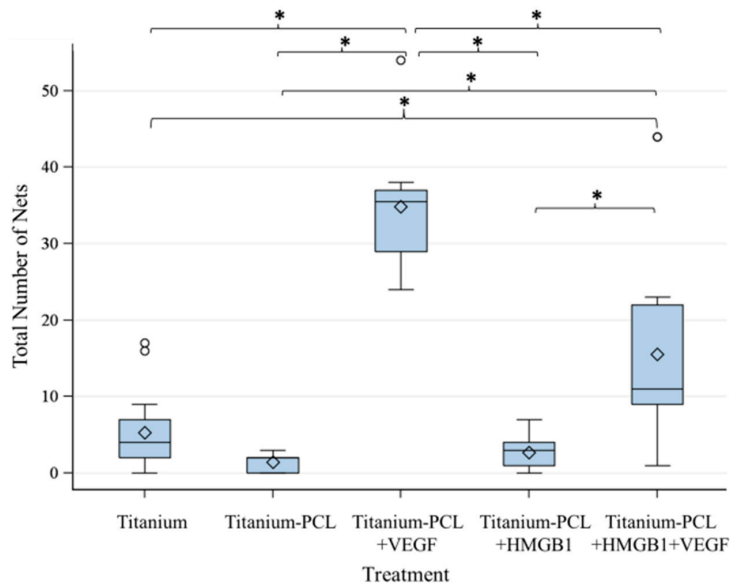


**Figure 7.** Number of Nets built by investigated implants. VEGF-functionalized titanium-PCL implants lead to significantly more building of net-like structures than all of the other titanium implants with or without cytokines in the assay. VEGF + HMGB1-functionalized titanium-PCL implants built significantly more nets than pure titanium implants, titanium-PCL implants and HMGB1-functionalized titanium-PCL implants. *F*-test from the analysis of variance followed by pairwise multiple means comparisons with the Least Significant Difference test were used ( $p \leq 0.05$ ).

2.4. Angiogenesis Assay with Cytokines HMGB1 and VEGF

Angiogenesis assay was also performed with cytokines to rule out any effects of the implant and coating materials. The parameters Junctions, Number of Tubules, Total Tubule Length and Number of Nets were compared in order to determine the effect of the different cytokine concentrations (Figure 8). Controls were run with the assay as previously described and showed significant differences between each other, being proof of concept for this onset. VEGF being inserted into the assay at the different medium changes at a steady concentration of 10 ng/mL significantly showed the best angiogenesis stimulating results. VEGF being inserted into the assay at the different medium changes according to the concentrations in the table in Section 4.6 also showed a significant angiogenesis stimulating effect. In contrast, HMGB1 did not show any angiogenesis stimulating effect at all. Results were similar to those of the controls with medium only and with suramin.

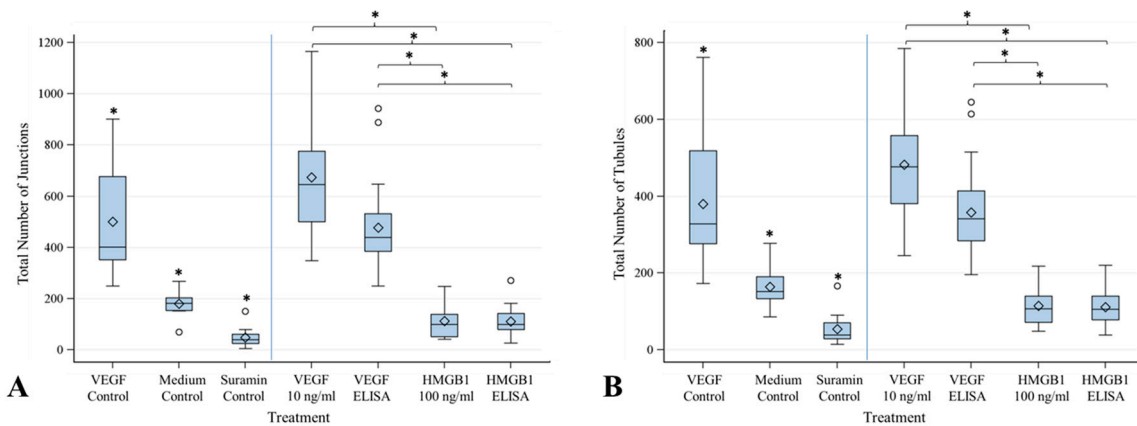


**Figure 8.** Cont.

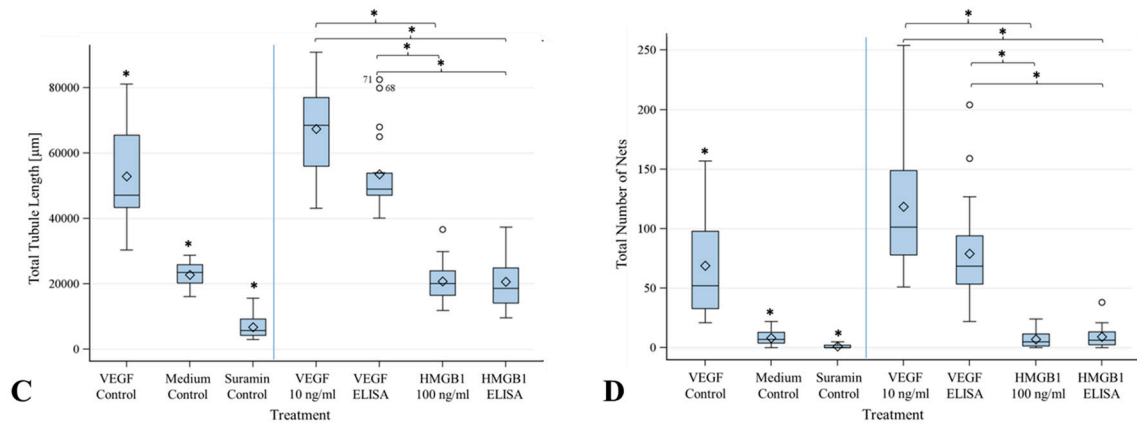


**Figure 8.** Results of Angiogenesis Assay with proangiogenic cytokines VEGF and HMGB1. Angiogenesis Assay with VEGF at a steady concentration of 10 ng/mL ( $n = 4$ ) and a declining concentration of 117 ng/mL on day 2, 16 ng/mL on day 5, 7 ng/mL on day 8 and 6 ng/mL on day 11 ( $n = 4$ ), respectively. HMGB1 was used at a steady concentration of 100 ng/mL ( $n = 4$ ) and a declining concentration of 924 ng/mL at day 2, 130 ng/mL at day 5, 76 ng/mL at day 8 and 24 ng/mL at day 11, respectively. Results for Total Number of Junctions (A); Total Number of Tubules (B); Total Tubule Length ( $\mu\text{m}$ ) (C); and Total Number of Nets (D) were analyzed using *F*-test from the analysis of variance followed by pairwise multiple means comparisons with the use of the Least Significant Difference ( $p \leq 0.05$ ). Both, VEGF using a concentration of 10 ng/mL and the declining concentrations, showed an angiogenesis stimulating effect. The steady concentration of 10 ng/mL showed significantly more tubules and junction formation than the declining concentrations. Neither the constant concentration of 100 ng/mL HMGB1 nor the declining concentrations of HMGB1 showed an angiogenesis stimulating effect.

### 2.5. Factor Releasing Amounts of Functionalized Titanium Implants

Releasing kinetics of functionalized implants used in the angiogenesis assay were analyzed using commercial ELISA-kits (RayBio<sup>®</sup> Human VEGF-A ELISA Kit, RayBiotech, Norcross, GA, USA) and HMGB1 ELISA Kit II, Shino-Test Corporation, Kanagawa, Japan). The ELISA results displayed in Tables 2 and 3 as well as in Figures 9 and 10 show a burst release of cytokines from the PCL coating.

**Table 2.** Releasing kinetics of HMGB1. Results of HMGB1 ELISA. Concentrations of HMGB1 released by scaffolds functionalized with HMGB1 (HMGB1\_1 to HMGB1\_3), respectively with a combination of VEGF and HMGB1 (VEGF + HMGB1\_1 to VEGF + HMGB1\_3) were measured at different points in time using sandwich ELISA in (ng/mL).

Concentration of HMGB1 (ng/mL)	Day 5	Day 8	Day 11	Day 14
HMGB1_1	858	89	27	19
HMGB1_2	991	173	49	28
HMGB1_3	>1678	316	152	107
VEGF + HMGB1_1	1477	110	41	26
VEGF + HMGB1_2	1655	228	37	27
VEGF + HMGB1_3	1479	121	29	19



**Table 3.** Releasing kinetics of VEGF. Results of VEGF ELISA. Concentrations VEGF released by scaffolds functionalized with VEGF (VEGF\_1 to VEGF\_3), respectively with a combination of VEGF and HMGB1 (VEGF + HMGB1\_1 to VEGF + HMGB1\_3) were measured at different points in time using sandwich ELISA in (ng/mL).

Concentration of VEGF (ng/mL)	Day 5	Day 8	Day 11	Day 14
VEGF_1	118	19	9	6
VEGF_2	139	15	6	3
VEGF_3	93	16	7	5
VEGF + HMGB1_1	101	8	9	1
VEGF + HMGB1_2	127	23	2	1
VEGF + HMGB1_3	134	6	2	1

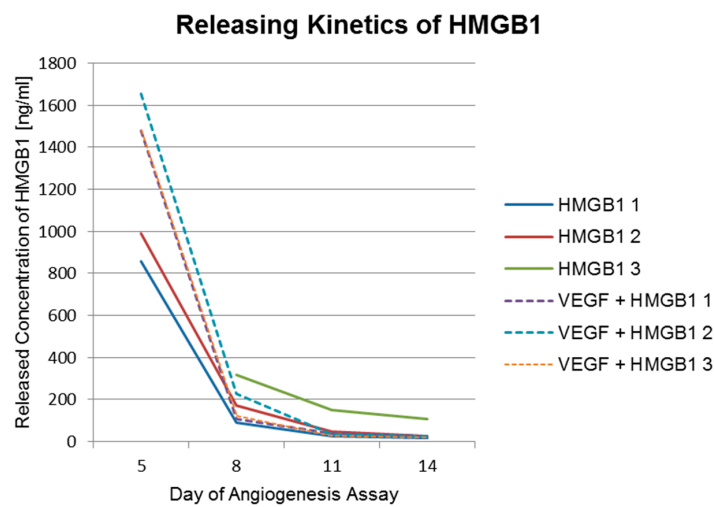


**Figure 9.** Released amounts of HMGB1. Releasing kinetics of HMGB1 from titanium implants coated with PCL and functionalized with HMGB1 and from titanium implants coated with PCL and functionalized with VEGF and HMGB1 (dashed lines). The concentration of HMGB1 released from titanium PCL scaffold HMGB1 3 (green line) was above the detection limit of 1668 ng/mL at day 5. Therefore, no result for this day can be shown.

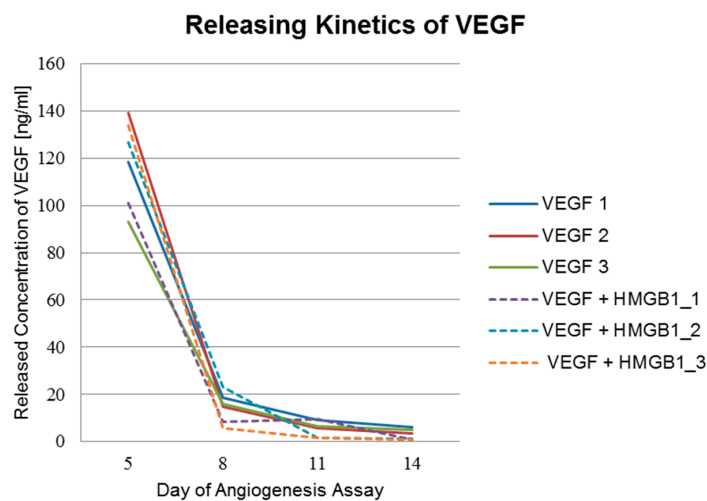


**Figure 10.** Released amounts of VEGF. Releasing kinetics of VEGF from titanium implants coated with PCL and functionalized with VEGF and from titanium implants coated with PCL and functionalized with VEGF and HMGB1 (dashed lines).

### 3. Discussion

Supernatants from titanium implants functionalized with VEGF and/or HMGB1 showed significantly higher chemotactic attraction for GM7373 compared to the starvation medium or 20% DMEM. VEGF is a well-known proangiogenic factor and HMGB1 has also been proven to induce migration of GM7373 [30]. Both cytokines were comparatively evaluated in previous studies and HMGB1 was found to be the more potent chemoattractive factor for GM7373 [31]. The aim of the onset was to prove that cytokines diffused out of the PCL layer of titanium implants are still bioactive and able to induce migration. The results show that VEGF as well as HMGB1 are still functional after incorporation into PCL coated titanium implants. Released concentrations are sufficient to induce chemotactic effects. There was no significant difference between VEGF and HMGB1, but VEGF alone was slightly better than the combination of VEGF and HMGB1. Adsorption and releasing kinetics of these cytokines into and from PCL-coated titanium implants are not well known yet.

Tubuli formation and building of junctions as well as nets was visible using titanium implants coated with PCL and functionalized with both, VEGF and a combination of VEGF and HMGB1. VEGF lead to significantly more tubuli formation than the combination of both factors. This could be due to interactions between VEGF and HMGB1 during adsorption and releasing, resulting in higher released concentrations of HMGB1 when both cytokines are incorporated. Furthermore, different signal pathways were activated in cells, which maybe act antagonistically, because the same amount of VEGF was released like in VEGF only-loaded scaffolds. As HMGB1 alone did not have any effect or show more sprouting than pure titanium implants or titanium implants coated with PCL, it can be assumed that the released concentration of HMGB1 failed to stimulate cells used in this assay. Another possibility might be that HMGB1 does not stimulate cells under these assay conditions at all.

To rule out any negative impact of the implant in combination with the cytokines, a second angiogenesis assay was performed with cytokines dissolved in the cell culture media. In this, a constant concentration of each cytokine was compared to the declining concentrations released during the first angiogenesis assay. VEGF at a constant concentration of 10 ng/mL reached the best angiogenesis stimulating results. This concentration has also been proven to stimulate migration of endothelial cells [31]. It was even significantly better than the positive control in this assay (VEGF at a concentration of 2 ng/mL). Nevertheless, VEGF at declining concentrations (117 ng/mL, 16 ng/mL, 7 ng/mL, 5 ng/mL) was significantly more stimulating than the controls (cell culture medium without supplements) and HMGB1, both at a constant concentration of 100 ng/mL and at a declining concentration (924 ng/mL, 130 ng/mL, 76 ng/mL, 24 ng/mL). In fact, neither the constant concentration nor the declining concentrations of HMGB1 lead to any stimulation of angiogenesis recognisable by similar results to the controls of the assay (medium without supplements and negative control with suramin). In a previous study, it was shown that the interaction between HMGB1 and its receptor RAGE does not have any effect on neovascularization in the fibroblast growth-factor mediated angiogenesis pathway [32]. This might be a reason for the failure of HMGB1 in this assay. Otherwise, the added concentration of 100 ng/mL could be insufficient for this onset. This concentration was tested by Matena *et al.* and found to be chemotactic for endothelial cells [31]. Best angiogenetic effects in an *in vitro* spheroid model were reached at a concentration of 2 µg/mL HMGB1 [28].

However, pure titanium implants lead to better results than titanium implants coated with PCL. Although PCL is proven to enable cell growth and proliferation on its surface [18], it seems to have a negative impact on angiogenesis. PCL is used as material for coronary stents and thus proven to be biocompatible but still should not promote vessel ingrowth in this application [33]. PCL might not be the perfect material for our investigation, but it has been proven to stimulate angiogenesis when VEGF has been incorporated. Therefore, titanium implants coated with PCL as a local drug delivery device are adequate, but it should also be taken into consideration to investigate more suitable polymers for angiogenesis in future.

Results show a fast initial release of the cytokines. This burst release indicates that most of the cytokines adsorb to the polymer surface. The released concentrations measured three days after insertion of the implants into the assay (day 5 of the assay) were 10-fold higher than following concentrations (10 ng/mL for VEGF and 100 ng/mL for HMGB1, respectively). The released concentrations at day 5 of the assay of HMGB1 from scaffolds functionalized with HMGB1 range from 858 ng/mL to above 1678 ng/mL. 1678 ng/mL was the highest measurable concentration and was exceeded by one of the scaffolds. At day 8 of the assay, concentrations ranged from 89 ng/mL to 316 ng/mL. Huge differences were also visible at day 11 and day 14 of the assay as shown in Table 2. This indicates that the cytokines also diffuse into deeper layers of the polymer. Besides, another reason for the vast differences between the single scaffolds releasing amounts of VEGF and HMGB1 might be an uneven PCL coating thickness of the titanium scaffolds.

A larger amount of HMGB1 is released using titanium PCL scaffolds functionalized with both cytokines. On occasions, this might be explained by the competitive protein exchange. It was first observed in 1960 and is now commonly referred to as the “Vroman effect” [34,35]. In a first step, abundant proteins of high concentrations and a lower affinity adsorb reversibly to the surface. Later, scarcer proteins of higher affinity displace the preadsorbed protein [36]. Another possible exchange process, which describes adsorption and desorption of protein molecules on surfaces postulates that, besides the concentration, also proteins with smaller molecular mass adsorb first to the surface. Proteins with a larger molecular mass embed themselves into the previously adsorbed protein and build a transient complex [37]. Probably HMGB1 with a molecular mass of 21 kDa and a higher loading concentration (200 µg/mL) bound to the PCL surface first. In a second step, the larger VEGF molecules with a mass of 46 kDa and a lower loading concentration (20 µg/mL) bound to the HMGB1 layer and built a transient complex. This complex turns upside down as VEGF has a higher adsorption energy due to its higher molecular mass. HMGB1 forms a layer on the VEGF and additionally fills the gaps on the PCL surface, which cannot be filled by VEGF because of its size. Nevertheless, releasing behavior is similar with a quick initial release, reaching a plateau afterwards. The initial release even seems to be slightly higher and faster when both cytokines are incorporated. This could be due to interference between VEGF and HMGB1 during the release from the PCL coating by the “transient complex” model [37].

## 4. Materials and Methods

### 4.1. Cell Culture

GM7373 is an endothelial cell line derived from the aorta of a bovine calf (kindly provided by Prof. Dr. Anaclet Ngezahayo, Leibniz University, Institution of Biophysics, Hannover, Germany).

The cells were cultured under standard conditions in DMEM medium (Biochrom AG, Berlin, Germany) with 10% fetal calf serum (FCS) at 37 °C and 5% CO<sub>2</sub>.

### 4.2. PCL Coating of Titanium Implants and Characterization

Coating was performed as described elsewhere [18]. The quality of surface morphology of the PCL coatings was checked by environmental scanning electron microscopy (Quanta FEG 250, FEI, Eindhoven, The Netherlands) before and after *in vitro* studies. Furthermore, cross-section polishes of PCL coated titanium implants were prepared after *in vitro* studies to determine the thickness of the PCL coating ( $n = 3$ ). For this purpose, we performed several measurements at different positions regarding the scaffold area and cross-section position with a minimum of 30 checkpoints. Washed and dried coated titanium implants were also weighed to determine the PCL mass of coatings with a special accuracy balance (UMX 5 Mettler Toledo, Greifensee, Switzerland,  $n = 5$ ). Procedures were performed according to Matena *et al.* [38].

#### 4.3. Incorporation of VEGF and HMGB1 into Titanium Implants

Titanium implants were produced as previously described [18] and coated by the Institute for Biomedical Engineering, Rostock University Medical Center, Rostock, Germany. Scaffolds were sanitized using fumigation with ethylene oxide, and all operations were performed under laminar flow. Human VEGF (450-32, Peprotech, Hamburg, Germany) and HMGB1 (H4652, Sigma-Aldrich, Taufkirchen, Germany) were incorporated in polymer coatings by sorption. The sorption of VEGF (20 µg/mL) and HMGB1 (200 µg/mL) and both supplements in combination (VEGF 20 µg/mL + HMGB1 200 µg/mL) took place in aseptic filtered sodium carbonate buffer (0.05 M, pH 9.6) at 37 °C for 24 h on a shaker.

#### 4.4. Migration Assay of GM7373 on Functionalized Titanium PCL Implants

Implants functionalized with VEGF ( $n = 9$ ), HMGB1 ( $n = 9$ ) and the combination of both cytokines ( $n = 9$ ) were immersed into serum-free DMEM (Biochrom AG, Berlin, Germany) and incubated for 24 h at 37 °C with 5% CO<sub>2</sub>. Supernatants of three implants were each pooled and collected. 70,000 GM7373 cells of passage P 22 were seeded onto 12-well transwells (353182, BD Falcon, Erembodegem, Belgium) with 8 µm pore-size, which were inserted into DMEM with 0.1% fetal calf serum (FCS) (PAA, Coelbe, Germany) and preheated at 37 °C and 5% CO<sub>2</sub> for 30 min. 0.1% DMEM under the transwells was replaced by the supernatants of functionalized implants in triplicate. 0.1% DMEM ( $n = 3$ ) and 20% DMEM ( $n = 3$ ) served as negative controls. Cells that did not migrate after 75 min were removed from the upper side of the transwells using a cotton stick. Migrated cells at the bottom site of the transwells were washed with Phosphate Buffered Saline (PBS) (Biochrom AG, Berlin, Germany), fixed with ice-cold methanol (AppliChem, Darmstadt, Germany) and stained with 1% crystal violet (Sigma Aldrich, Munich, Germany). Five pictures at different positions of each transwell were taken at a magnification of 40x using Live Cell Imaging Microscope (DMI6000B, Leica Microsystems, Wetzlar, Germany) with the program LAS V4A, and migrated cells were counted.

#### 4.5. Angiogenesis Assay with Functionalized Titanium PCL Implants

In order to investigate the impact of functionalized implants on tubulus formation *in vitro*, V2a Kit™—Vasculogenesis to Angiogenesis (TCSCellworks, Buckingham, UK)—was performed according to the protocol provided by the manufacturer [39]. The kit supplies growing co-cultures of human matrix and endothelial cells in a 24 well plate format.

V2a Co-Culture Cells (TCSCellworks, Buckingham, UK) were thawed in V2a Seeding Medium (TCSCellworks, Buckingham, UK), seeded evenly in a 24-well plate and incubated at 37 °C with 5% CO<sub>2</sub>. After 24 h, the medium was changed to V2a Growth Medium (TCSCellworks, Buckingham, UK) and test compounds added. Controls were performed according to the manufacturer's recommendations in order to verify the results of the assay. Different implant materials with and without coating and proangiogenic factors were tested as compounds. Pure titanium scaffolds ( $n = 3$ ) and PCL coated titanium scaffolds ( $n = 3$ ) were each placed in one well. Titanium implants coated with PCL and functionalized with VEGF ( $n = 3$ ) and HMGB1 ( $n = 3$ ) were added as well as titanium PCL implants functionalized with VEGF and HMGB1 in combination ( $n = 3$ ). Every 72 h, co-cultures were examined microscopically and medium was changed carefully to avoid movement of the implant according to the protocol. Supernatants were collected and stored at −20 °C for further experiments.

After 14 days, cells were washed with Phosphate Buffered Saline (PBS) (Biochrom AG, Berlin, Germany), fixed with 70% ice-cold ethanol (AppliChem, Darmstadt, Germany) and stained with mouse anti-human CD31 primary antibody and goat anti-mouse IgG AP conjugate secondary antibody according to the protocol provided by TCSCellworks. In a final step, staining was performed using 5-bromo-4-chloro-3-indolyl-phosphate/nitro blue tetrazolium (BCIP/NBT) (TCSCellworks, Buckingham, UK). Pictures of cells were taken at five different determined fields (four evenly spread

in the border area and one in the middle next to the implant) at  $\times 40$  magnification using Live Cell Imaging Microscope (DMI6000B, Leica Microsystems, Wetzlar, Germany) with the program LAS V4A.

By using the software ImageJ (Wayne Rasband, National Institutes of Health, Bethesda, MD, USA), pictures were processed and tubule formation was analyzed with the help of Cellworks Image Analysis Software, *AngioSys 2.0* (TCSCellworks, Buckingham, UK).

#### 4.6. Angiogenesis Assay with Cytokines VEGF and HMGB1

Another Angiogenesis Assay was performed as described above. VEGF and HMGB1 were added at concentrations according to releasing kinetics of functionalized titanium implants ( $n = 4$  for VEGF and  $n = 4$  for HMGB1) with medium changes every 72 h. As the measured concentrations had changed over the period of 14 days, different concentrations were added at each medium change. Added concentrations are shown in Table 4. These concentrations were compared to steady concentration of VEGF (10 ng/mL) ( $n = 4$ ) and HMGB1 (100 ng/mL) ( $n = 4$ ).

**Table 4.** Cytokine concentrations. Cytokine concentrations of VEGF and HMGB1 added to the angiogenesis assay at different points in time.

Points in Time	VEGF (ng/mL)	HMGB1 (ng/mL)
Concentration added at day 2	117	924
Concentration added at day 5	16	130
Concentration added at day 8	7	76
Concentration added at day 11	5	24

#### 4.7. Factor Releasing Kinetics of Functionalized Titanium Implants

A specific VEGF sandwich-ELISA using RayBio<sup>®</sup> Human VEGF-A ELISA Kit (RayBiotech, Norcross, GA, USA) and a specific HMGB1 sandwich-ELISA (HMGB1 Elisa Kit II, Shino-Test Corporation, Kanagawa, Japan) were performed with supernatants from Angiogenesis Assay of functionalized titanium implants. Supernatants were taken 3, 6, 9, and 12 days, respectively after insertion of functionalized titanium implants into the Angiogenesis Assay and stored at  $-20\text{ }^{\circ}\text{C}$ .

## 5. Conclusions

VEGF and HMGB1 maintain their chemotactic effect on endothelial cells after being released from functionalized PCL-coated titanium implants.

VEGF-functionalized PCL-coated titanium implants were proven to act also proangiogenically in the V2a Kit<sup>TM</sup>, whereas HMGB1-functionalized PCL-coated titanium implants did not have any proangiogenic effect.

A burst release could be observed when evaluating the releasing profile of functionalized implants, indicating that the major amount of the cytokines is located at the polymer surface.

**Acknowledgments:** The authors would kindly like to thank Anaclet Ngezahayo from Leibniz University, Institution of Biophysics, Hannover, Germany for providing the GM7373 cell line and the Deutsche Forschungsgemeinschaft (DFG, German Research Foundation) for their funding and support of the project listed under support code No. 299/11-1.

**Author Contributions:** Ingo Nolte, Hugo Murua Escobar, Heinz Haferkamp, and Nils-Claudius Gellrich performed the primary study design, manuscript editing, and made final improvements. Laura Roland, Samantha Backhaus, Michael Grau, and Michael Teske performed experiments. Laura Roland, Michael Teske, and Martin Beyerbach analyzed the data. Laura Roland, Michael Teske, and Martin Beyerbach wrote the manuscript.

**Conflicts of Interest:** The authors declare no conflict of interest. The founding sponsors had no role in the design of the study, in the collection, analyses, or interpretation of data, in the writing of the manuscript, or in the decision to publish the results.

## References

1. Saran, U.; Gemini Piperni, S.; Chatterjee, S. Role of angiogenesis in bone repair. *Arch. Biochem. Biophys.* **2014**, *561*, 109–117. [[CrossRef](#)] [[PubMed](#)]
2. Carano, R.A.; Filvaroff, E.H. Angiogenesis and bone repair. *Drug Discov. Today* **2003**, *8*, 980–989. [[CrossRef](#)]
3. Kanczler, J.M.; Oreffo, R.O. Osteogenesis and angiogenesis: The potential for engineering bone. *Eur. Cells Mater.* **2008**, *15*, 100–114.
4. Einhorn, T.A. Enhancement of fracture-healing. *J. Bone Jt. Surg. Am. Vol.* **1995**, *77*, 940–956.
5. Guo, J.; Meng, Z.; Chen, G.; Xie, D.; Chen, Y.; Wang, H.; Tang, W.; Liu, L.; Jing, W.; Long, J.; *et al.* Restoration of critical-size defects in the rabbit mandible using porous nanohydroxyapatite-polyamide scaffolds. *Tissue Eng. Part A* **2012**, *18*, 1239–1252. [[CrossRef](#)] [[PubMed](#)]
6. Rentsch, C.; Rentsch, B.; Breier, A.; Spekl, K.; Jung, R.; Manthey, S.; Scharnweber, D.; Zwipp, H.; Biewener, A. Long-bone critical-size defects treated with tissue-engineered polycaprolactone-co-lactide scaffolds: A pilot study on rats. *J. Biomed. Mater. Res. Part A* **2010**, *95*, 964–972. [[CrossRef](#)] [[PubMed](#)]
7. Xu, L.; Lv, K.; Zhang, W.; Zhang, X.; Jiang, X.; Zhang, F. The healing of critical-size calvarial bone defects in rat with rhPDGF-BB, BMSCs, and  $\beta$ -TCP scaffolds. *J. Mater. Sci. Mater. Med.* **2012**, *23*, 1073–1084. [[CrossRef](#)] [[PubMed](#)]
8. Gellrich, N.C.; Held, U.; Schoen, R.; Pailing, T.; Schramm, A.; Bormann, K.H. Alveolar zygomatic buttress: A new donor site for limited preimplant augmentation procedures. *J. Oral Maxillofac. Surg.* **2007**, *65*, 275–280. [[CrossRef](#)] [[PubMed](#)]
9. Goulet, J.A.; Senunas, L.E.; DeSilva, G.L.; Greenfield, M.L. Autogenous iliac crest bone graft. Complications and functional assessment. *Clin. Orthop. Relat. Res.* **1997**, *339*, 76–81. [[CrossRef](#)] [[PubMed](#)]
10. Silber, J.S.; Anderson, D.G.; Daffner, S.D.; Brislin, B.T.; Leland, J.M.; Hilibrand, A.S.; Vaccaro, A.R.; Albert, T.J. Donor site morbidity after anterior iliac crest bone harvest for single-level anterior cervical discectomy and fusion. *Spine* **2003**, *28*, 134–139. [[CrossRef](#)] [[PubMed](#)]
11. Li, J.P.; Li, S.H.; Van Blitterswijk, C.A.; de Groot, K. Cancellous bone from porous Ti6Al4V by multiple coating technique. *J. Mater. Sci. Mater. Med.* **2006**, *17*, 179–185. [[CrossRef](#)] [[PubMed](#)]
12. Niinomi, M. Mechanical biocompatibilities of titanium alloys for biomedical applications. *J. Mech. Behav. Biomed. Mater.* **2008**, *1*, 30–42. [[CrossRef](#)] [[PubMed](#)]
13. Van der Stok, J.; Van der Jagt, O.P.; Amin Yavari, S.; De Haas, M.F.; Waarsing, J.H.; Jahr, H.; Van Lieshout, E.M.; Patka, P.; Verhaar, J.A.; Zadpoor, A.A.; *et al.* Selective laser melting-produced porous titanium scaffolds regenerate bone in critical size cortical bone defects. *J. Orthop. Res.* **2013**, *31*, 792–799. [[CrossRef](#)] [[PubMed](#)]
14. Janssen, L.M.; van Osch, G.J.; Li, J.P.; Kops, N.; de Groot, K.; Von den Hoff, J.W.; Feenstra, L.; Hardillo, J.A. Tracheal reconstruction: Mucosal survival on porous titanium. *Arch. Otolaryngol. Head Neck Surg.* **2009**, *135*, 472–478. [[CrossRef](#)] [[PubMed](#)]
15. Loh, Q.L.; Choong, C. Three-dimensional scaffolds for tissue engineering applications: Role of porosity and pore size. *Tissue Eng. Part B Rev.* **2013**, *19*, 485–502. [[CrossRef](#)] [[PubMed](#)]
16. Zhu, K.; Li, C.; Zhu, Z.; Liu, C.S. Measurement of the dynamic Young's modulus of porous titanium and Ti6Al4V. *J. Mater. Sci.* **2007**, *42*, 7348–7353. [[CrossRef](#)]
17. Van der Stok, J.; Wang, H.; Amin Yavari, S.; Siebelt, M.; Sandker, M.; Waarsing, J.H.; Verhaar, J.A.; Jahr, H.; Zadpoor, A.A.; Leeuwenburgh, S.C.; *et al.* Enhanced bone regeneration of cortical segmental bone defects using porous titanium scaffolds incorporated with colloidal gelatin gels for time- and dose-controlled delivery of dual growth factors. *Tissue Eng. Part A* **2013**, *19*, 2605–2614. [[CrossRef](#)] [[PubMed](#)]
18. Roland, L.; Grau, M.; Matena, J.; Teske, M.; Gieseke, M.; Kampmann, A.; Beyerbach, M.; Murua Escobar, H.; Haferkamp, H.; Gellrich, N.C.; *et al.* Poly- $\epsilon$ -caprolactone coated and functionalized porous titanium and magnesium implants for enhancing angiogenesis in critically sized bone defects. *Int. J. Mol. Sci.* **2016**, *17*. [[CrossRef](#)] [[PubMed](#)]
19. Geiger, M.; Li, R.H.; Friess, W. Collagen sponges for bone regeneration with rhBMP-2. *Adv. Drug Deliv. Rev.* **2003**, *55*, 1613–1629. [[CrossRef](#)] [[PubMed](#)]
20. Lindhorst, D.; Tavassol, F.; von See, C.; Schumann, P.; Laschke, M.W.; Harder, Y.; Bormann, K.H.; Essig, H.; Kokemuller, H.; Kampmann, A.; *et al.* Effects of VEGF loading on scaffold-confined vascularization. *J. Biomed. Mater. Res. Part A* **2010**, *95*, 783–792. [[CrossRef](#)] [[PubMed](#)]

21. Müller, S.; Koenig, G.; Charpiot, A.; Debry, C.; Voegel, J.-C.; Lavalle, P.; Vautier, D. VEGF-functionalized polyelectrolyte multilayers as proangiogenic prosthetic coatings. *Adv. Funct. Mater.* **2008**, *18*, 1767–1775. [[CrossRef](#)]
22. Woodruff, M.A.; Hutmacher, D.W. The return of a forgotten polymer—Polycaprolactone in the 21st century. *Prog. Polym. Sci.* **2010**, *35*, 1217–1256. [[CrossRef](#)]
23. Lam, C.X.; Hutmacher, D.W.; Schantz, J.T.; Woodruff, M.A.; Teoh, S.H. Evaluation of polycaprolactone scaffold degradation for 6 months *in vitro* and *in vivo*. *J. Biomed. Mater. Res. Part A* **2009**, *90*, 906–919. [[CrossRef](#)] [[PubMed](#)]
24. Romagnoli, C.; Zonefrati, R.; Galli, G.; Puppi, D.; Piroso, A.; Chiellini, F.; Martelli, F.S.; Tanini, A.; Brandi, M.L. *In vitro* behavior of human adipose tissue-derived stem cells on poly( $\epsilon$ -caprolactone) film for bone tissue engineering applications. *BioMed Res. Int.* **2015**, *2015*. [[CrossRef](#)] [[PubMed](#)]
25. Sawyer, A.A.; Song, S.J.; Susanto, E.; Chuan, P.; Lam, C.X.; Woodruff, M.A.; Hutmacher, D.W.; Cool, S.M. The stimulation of healing within a rat calvarial defect by mPCL-TCP/collagen scaffolds loaded with rhBMP-2. *Biomaterials* **2009**, *30*, 2479–2488. [[CrossRef](#)] [[PubMed](#)]
26. Breier, G.; Risau, W. The role of vascular endothelial growth factor in blood vessel formation. *Trends Cell Biol.* **1996**, *6*, 454–456. [[CrossRef](#)]
27. Ferrara, N. Vascular endothelial growth factor: Basic science and clinical progress. *Endocr. Rev.* **2004**, *25*, 581–611. [[CrossRef](#)] [[PubMed](#)]
28. Schlueter, C.; Weber, H.; Meyer, B.; Rogalla, P.; Roser, K.; Hauke, S.; Bullerdiek, J. Angiogenetic signaling through hypoxia: HMGB1: An angiogenetic switch molecule. *Am. J. Pathol.* **2005**, *166*, 1259–1263. [[CrossRef](#)]
29. Van Beijnum, J.R.; Buurman, W.A.; Griffioen, A.W. Convergence and amplification of toll-like receptor (TLR) and receptor for advanced glycation end products (RAGE) signaling pathways via high mobility group B1 (HMGB1). *Angiogenesis* **2008**, *11*, 91–99. [[CrossRef](#)] [[PubMed](#)]
30. Mitola, S.; Belleri, M.; Urbinati, C.; Coltrini, D.; Sparatore, B.; Pedrazzi, M.; Melloni, E.; Presta, M. Cutting edge: Extracellular high mobility group box-1 protein is a proangiogenic cytokine. *J. Immunol.* **2006**, *176*, 12–15. [[CrossRef](#)] [[PubMed](#)]
31. Matena, J.; Petersen, S.; Gieseke, M.; Kampmann, A.; Teske, M.; Beyerbach, M.; Murua Escobar, H.; Haferkamp, H.; Gellrich, N.C.; Nolte, I. SLM produced porous titanium implant improvements for enhanced vascularization and osteoblast seeding. *Int. J. Mol. Sci.* **2015**, *16*, 7478–7492. [[CrossRef](#)] [[PubMed](#)]
32. Taguchi, A.; Blood, D.C.; del Toro, G.; Canet, A.; Lee, D.C.; Qu, W.; Tanji, N.; Lu, Y.; Lalla, E.; Fu, C.; *et al.* Blockade of rage-amphoterin signalling suppresses tumour growth and metastases. *Nature* **2000**, *405*, 354–360. [[PubMed](#)]
33. Flege, C.; Vogt, F.; Hoges, S.; Jauer, L.; Borinski, M.; Schulte, V.A.; Hoffmann, R.; Poprawe, R.; Meiners, W.; Jobmann, M.; *et al.* Development and characterization of a coronary polylactic acid stent prototype generated by selective laser melting. *J. Mater. Sci. Mater. Med.* **2013**, *24*, 241–255. [[CrossRef](#)] [[PubMed](#)]
34. Vroman, L.; Adams, A.L. Findings with the recording ellipsometer suggesting rapid exchange of specific plasma proteins at liquid/solid interfaces. *Surf. Sci.* **1969**, *16*, 438–446. [[CrossRef](#)]
35. Vroman, L.; Adams, A.L. Identification of rapid changes at plasma-solid interfaces. *J. Biomed. Mater. Res.* **1969**, *3*, 43–67. [[CrossRef](#)] [[PubMed](#)]
36. Kim, J.-H. Protein adsorption on polymer particles. In *Encyclopedia of Surface and Colloid Science*; Somasundaran, P., Ed.; CRC Press: Boca Raton, FL, USA, 2004; Volume 5, pp. 519–523.
37. Hirsh, S.L.; McKenzie, D.R.; Nosworthy, N.J.; Denman, J.A.; Sezerman, O.U.; Bilek, M.M. The vroman effect: Competitive protein exchange with dynamic multilayer protein aggregates. *Colloids Surf. B Biointerfaces* **2013**, *103*, 395–404. [[CrossRef](#)] [[PubMed](#)]
38. Matena, J.; Petersen, S.; Gieseke, M.; Teske, M.; Beyerbach, M.; Kampmann, A.; Murua Escobar, H.; Gellrich, N.C.; Haferkamp, H.; Nolte, I. Comparison of selective laser melted titanium and magnesium implants coated with PCL. *Int. J. Mol. Sci.* **2015**, *16*, 13287–13301. [[CrossRef](#)] [[PubMed](#)]
39. V2a Kit Protocol. Available online: <http://www.cellworks.co.uk/v2akit.php> (accessed on 1 August 2015).

